Hydroxylation of cyclohexane catalyzed by iron(III)–iron(III) porphyrin dimers and DABCO with molecular oxygen: evidence for the conformation effect of porphyrin dimers on the catalytic activity

Qi-Zhi Ren, Jin-Wang Huang [1], Xiao-Bin Peng, Liang-Nian Ji [*]

School of Chemistry and Chemical Engineering, Zhongshan (Sun Yatsen) University, Canton 510275, China

Abstract

A series of p/p type iron(III)–iron(III) porphyrin dimers and corresponding zinc(II)–zinc(II) porphyrin dimers covalently linked by a flexible alkoxy chain ($-O(CH_2)_nO-$, $n = 2–10$) have been synthesized and characterized. The hydroxylation of cyclohexane catalyzed by iron(III)–iron(III) porphyrin dimers with molecular oxygen under mild conditions are reported, 1 eq. of bidentate ligand DABCO (1,4-diazobicyclo[2,2,2] octane) is added exactly as axial ligand to the catalytic system. The catalytic activities of these dimers are supposed to be related to the special conformations formed by porphyrin dimers and DABCO. By using ^{1}H-NMR, the conformation equilibrium of corresponding zinc(II)–zinc(II) porphyrin dimers and their binding behavior with 1 eq. DABCO has been discussed in detail. It has been proven that the higher catalytic activities of the catalytic system mainly result from the formation of the ternary sandwich complexes of iron(III)–iron(III) porphyrin dimers with DABCO. © 1999 Elsevier Science B.V. All rights reserved.

Keywords: Iron(III)–iron(III) porphyrin dimer; Hydroxylation; Conformation

1. Introduction

Metal dimers of porphyrins and related macrocyclic tetrapyrroles play important biological roles in the photosynthesis, catalysis and photoconduction, which derive from their remarkable electron transfer, energy transfer and special conformation properties [1–4]. Metalloporphyrin-catalyzed hydrocarbon oxidation is an important topic both to understand the catalytic mechanism of cytochrome *p*-450 monooxygenases and to find new efficient catalysts. We have reported previously that a series of iron (III)–metal-free porphyrin dimers covalently linked by flexible alkoxy chain were used as mimic cytochrome *p*-450 catalytic system and have discussed the effect of the steric hindrance caused by the equilibrium conformation of the porphyrin dimers and the intramolecular interaction between the two porphyrin rings [5,6].

* Corresponding author. Fax: +86-20-8418-4737; E-mail: cesjln@zsulink.zsu.edu.cn

[1] Also corresponding author.

In order to look for the new and direct evidence for the conformation effect of metalloporphyrin dimers on their catalytic activities, a series of p/p type iron(III)–iron(III) porphyrin dimers and their corresponding zinc(II)–zinc(II) porphyrin dimers covalently linked by flexible alkoxy chain ($-O(CH_2)_nO-$, $n = 2$–10) (Fig. 1) were synthesized. The iron(III)–iron(III) dimers were used as the catalysts of cyclohexane hydroxylation, a rigid bidentate ligand DABCO (1,4-diazobicyclo[2,2,2]octane) was added to the catalytic system as axial ligand with the 1:1 [porphyrin]/[DABCO] molar ratio, the catalytic results were discussed with the effect of special conformations formed by the dimers and DABCO. By using NMR spectroscopy, the conformation equilibrium of corresponding zinc(II)–zinc(II) porphyrin dimers has been discussed. It has been shown that with the increase of the length of alkoxy chain, the conformation equilibrium of the binuclear porphyrin dimers moves from open to closed conformation. The ^{1}H-NMR studies of the binding behavior of zinc(II)–zinc(II) porphyrin dimers and DABCO with 1/1 molar ratio have also been discussed, indicating that the higher catalytic activities of iron(III)–iron(III) porphyrin dimers are related to the special conformation formed by porphyrin dimers and DABCO.

2. Experimental

2.1. Preparation of the porphyrin dimers

The porphyrin dimers were synthesized as in the literature [7,8] and iron(III)–iron(III) porphyrin dimers were characterized by EA, FAB-MS, UV-VIS, IR and ESR. The zinc(II)–zinc(II) porphyrin dimers were characterized by EA, FAB-MS, UV-VIS, IR, ^{1}H-NMR and ^{1}H $-$ ^{1}H COSY.

2.2. Composition of catalytic system

Catalyst: iron(III)–iron(III) porphyrin dimer 0.01 mmol; reductant: zinc powder 1.5 mmol, acetic acid 0.80 mmol; axial ligand: DABCO 0.01 mmol; substrate: cyclohexane 5.55 mmol; solvent: 10 ml, MeCN:CH_2Cl_2 = 9:1.

The above system of imitative *P*-450 monooxygenase was carried out in a specially constructed reaction vessel at $30.0 \pm 0.2°C$ for 0.5 h, pure oxygen (101.3 kPa) was passed into the solution through the inlet value with magnetic stirring, the products were detected and quantitatively analyzed by gas chromatography (chlorobenzene was used as the internal standard) which were performed on a Shimadzu GC-9A gas chromatography coupled to a Shimadzu CR3-A integrator.
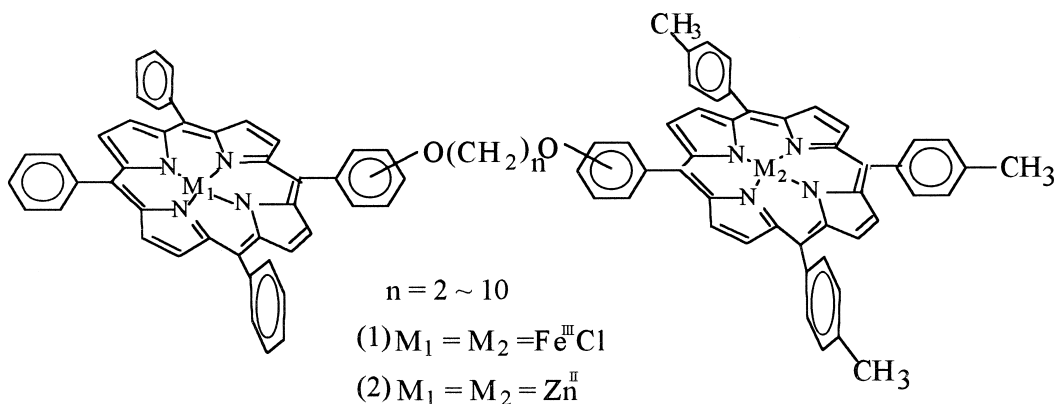

Fig. 1. Structure of p/p type iron(III)–iron(III) porphyrin dimers and corresponding zinc(II)–zinc(II) porphyrin dimers (1) C_nFe_2D, (2) C_nZn_2D.

2.3. ^{1}H-NMR study

Some 500 MHz ^{1}H-NMR and ^{1}H$-$^{1}H COSY spectra were recorded on UNITY INOVA 500NB (Varian) spectrometer. One-dimensional spectra were typically acquired by using 32 K data points over 5000 Hz spectra width, double precision was used, number of increments was 512, transient power was 53. For ^{1}H$-$^{1}H COSY spectra, typically 2 K data points were used in f_1 and f_2, with a spectral width 5000 Hz in each dimension. Zero-filling was used in f_1 but not used in f_2 and suitable apodization was applied in processing spectra. The sample concentration was ca. 10^{-3} M in deuteriochloroform solution, the temperature was 30°C, TMS was used as the internal standard. DABCO in CDCl$_3$ solution was added to porphyrin solutions via a 25-μl syringe.

3. Results and discussion

3.1. Characterization of iron(III)–iron(III) porphyrin dimers and zinc(II)–zinc(II) porphyrin dimers

The results of EA and FAB-MS for porphyrin dimers are close to the calculated values. The UV-VIS spectra of the porphyrin dimers are in good with that of a 1:1 mixture of the monomers MTPP and MTTP (M = Fe^{III}Cl, Zn^{II}), except the Soret bands of the dimers have a slight red shift due to the intramolecular interaction of the two porphyrin rings. For IR spectra, comparing with the free-base porphyrin dimers, the most obvious change is the disappearance of ν_{N-H} (about 3320 cm^{-1}) and a strong band appears at 1000 cm^{-1}. ESR signals at apparent $g_{\parallel}$ and $g_{\perp}$ values observed for iron(III)–iron(III) porphyrin dimers in CH$_2$Cl$_2$ at 77 K reveal the existence of a high spin ferric ion ($S = 5/2$) state. By using ^{1}H NMR and ^{1}H$-$^{1}H COSY, signals attributed to the alkoxy chain of zinc(II)–zinc(II) porphyrin dimers (for C$_2$Zn$_2$D, δ_α 4.756 ppm; for C$_6$Zn$_2$D, δ_α 4.326
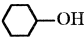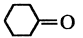
ppm, δ_β 2.090 ppm, δ_γ 1.836 ppm; for C$_{10}$Zn$_2$D, δ_α 4.254 ppm, δ_β 2.009 ppm, δ_γ 1.656 ppm, δ_δ 1.514 ppm) are discernible. All of these indicate that the porphyrin dimers covalently linked by alkoxy chain have been achieved.

3.2. Hydroxylation of cyclohexane catalyzed by iron(III)–iron(III) porphyrin dimers

The new model system is in the presence of zinc powder as reducing agent and acetic acid as proton source with molecular oxygen under mild condition, 1 eq. of bidentate ligand is added as axial ligand. catalytic results are listed in Table 1. It shows that the hydroxylation of cyclohexane catalyzed by iron(III)–iron(III) porphyrin dimers with DABCO as axial ligand has been achieved, the products are cyclohexanol and cyclohexanone. All the dimers have higher catalytic activities than corresponding monomer FeTPPCl under the same condition. Effect of the length of alkoxy chain on catalytic activities of porphyrin dimers and the monomer has been shown in Fig. 2. The total turnovers of C$_2$Fe$_2$D is 7.80, higher than that of FeTPPCl 5.02, with the increase of the length of alkoxy chain, the turnovers of C$_n$Fe$_2$D ($n = 4$, 6, 10) are much higher.

According to the theory about the catalytic cycle of cytochrome p-450, axial coordination of axial ligand to iron(III) porphyrin is very important for the activation of dioxygen. Only if the pentacoordinate high-spin iron(III) complex with the cysteinate as only axial ligand has formed and has been reduced, can it bind dioxygen and form the active high-valent species [Fe(V)=O] [9]. Although C$_n$Fe$_2$D dimers have two ferric centers, since the molar ratio [porphyrin]/[DABCO] is 1:1, just the same as the ratio of monomer, if the bidentate ligand binds only with one ferric center of these binuclear porphyrin dimers, their catalytic activities should be similar to that of monomer FeTPPCl. While from Table 1 and Fig. 2, it is obvious that the catalytic activities of porphyrin dimers are

Table 1
Catalytic activities of porphyrin dimers and their monomer FeTPPCl

Catalysts	Product	amount(mol×10^{-5})	Turnovers
	⬡—OH	⬡=O	(0.5hr)
FeTPPCl	3.11	1.91	5.02
C_2Fe_2D	4.58	3.22	7.80
C_4Fe_2D	8.91	5.32	14.23
C_6Fe_2D	10.60	6.61	17.21
$C_{10}Fe_2D$	10.23	6.65	16.88

Turnovers: cyclohexanol and cyclohexanone mol/catalyst (porphyrin) mol C_nFe_2D: iron(III)–iron(III) porphyrin dimer covalently linked by $-O(CH_2)_nO-$.

higher than that of monomer FeTPPCl and may be related to the special closed conformation of binuclear porphyrin dimers caused by the addition of 1 eq. DABCO.

It is well known that the equilibrium of two different conformations, open and closed, existed in porphyrin dimers in solution [10,11]. When the conformation of iron(III)–iron(III) porphyrin dimers exists in closed conformation (Fig. 3A), on the suitable condition, bidentate ligand DABCO can be inside the cavity of two porphyrin rings and bind with two ferric centers of porphyrin dimers, both ferric centers of porphyrin dimers become pentacoordinate complexes and have catalytic activities (Fig. 3B). After two ferric porphyrins have been reduced to ferrous complexes, dioxygen has possibility to be binded to the two Fe(II) porphyrins and two active high-valent species [Fe(V)=O] can be formed (Fig. 3C). It can be shown from
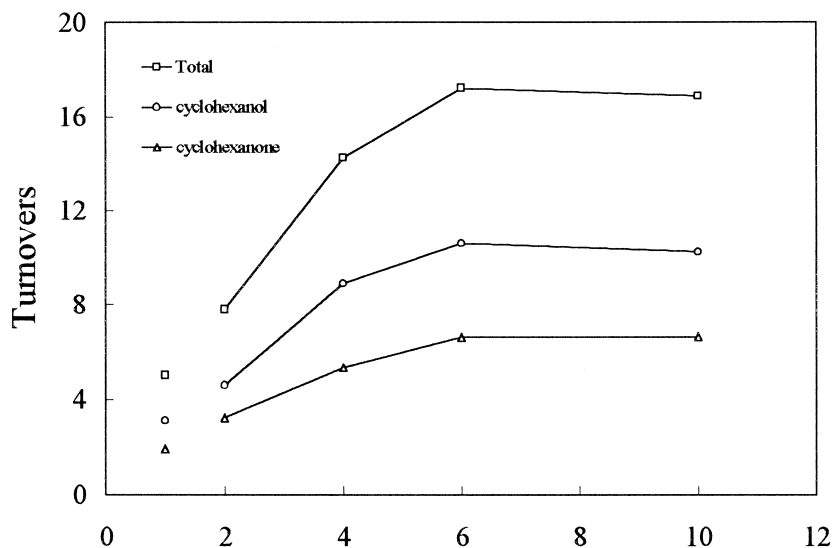

Fig. 2. Plots of the turnovers vs. carbon numbers of alkoxy chain, except turnovers of FeTPPCl are shown when abscissa is 1.
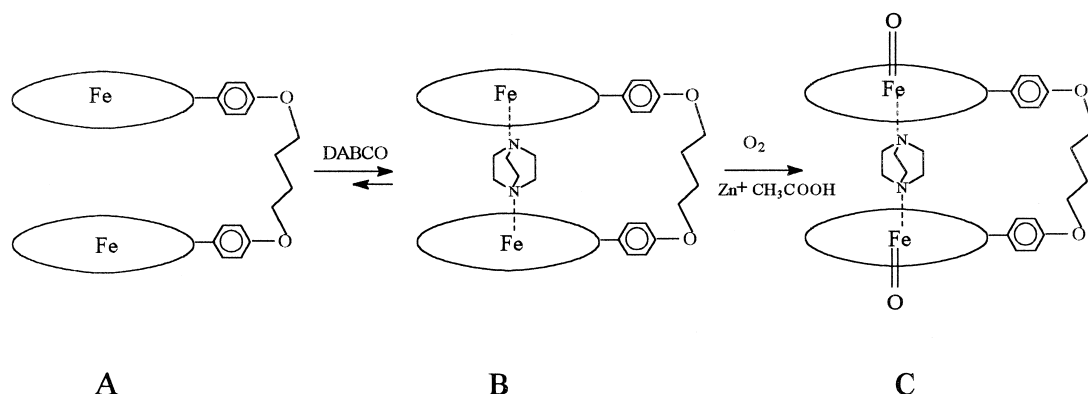
Fig. 3. The ternary DABCO–dimeric iron(III)-porphyrin complexation in the presence of 1 equiv. DABCO, dioxygen and reducing agent.

Table 1 that the order of catalytic activities for iron(III)–iron(III) porphyrin dimers is C_2Fe_2D < C_4Fe_2D < $C_6Fe_2D \approx C_{10}Fe_2D$. For C_2Fe_2D, it is difficult to form a stable ternary sandwich complex with DABCO since the tension caused by the short alkoxy chain is strong, so the catalytic activity of C_2Fe_2D is relatively low. With the increase of the length of alkoxy chain, the bidentate ligand can bind well with iron(III)–iron(III) dimers and form a stable 1/1 ternary adduct (Fig. 3B), both the ferric centers

of porphyrin dimers can have catalytic activities. Comparing with the catalytic activity of C_6Fe_2D, the slight decrease of the catalytic activity of $C_{10}Fe_2D$ may be related to the increased tension caused by the twist and fold of the long alkoxy chain. Furthermore, the steric hindrance caused by the cofacial ternary complex favors the formation of active $[Fe(V)=O]$ species, higher catalytic activity is gained by easier transfer of oxygen to cyclohexane, this steric hindrance can also repress the formation

Table 2
^{1}H NMR chemical shifts of zinc(II)–zinc(II) porphyrin dimers and DABCO (in ppm)

Signal	DABCO	$C_2Zn_2D^a$	$\Delta\delta_{C_2Zn_2D}{}^b$	C_6Zn_2D	$\Delta\delta_{C_6Zn_2D}$	$C_{10}Zn_2D$	$\Delta\delta_{C_{10}Zn_2D}$
meso-β_1		9.034	−0.079	9.011	−0.408	8.992	−0.399
β_2		9.014	−0.080	8.994	−0.409	8.971	−0.400
β_3		8.970	−0.084	8.955	−0.410	8.953	−0.402
phenyl 2′,6′		8.230	−0.032	8.210	−0.394	8.208	−0.384
tolyl 2″,6″		8.108	−0.035	8.094	−0.405	8.088	−0.396
2,6,		8.198	−0.036	8.146	−0.407	8.115	−0.397
2*,6*		8.183	−0.037	8.128	−0.407	8.094	−0.398
phenyl 3′-5′		7.748	−0.010	7.737	−0.104	7.735	−0.093
tolyl 3″,5″		7.546	−0.009	7.538	−0.100	7.534	−0.092
3,5		7.421	−0.007	7.319	−0.096	7.274	−0.087
3*,5*		7.405	−0.007	7.299	−0.088	7.255	−0.083
DABCO	2.791^c						
1:1 binding		1.520^d	−1.271^e	−4.727^d	−7.518^e	−4.815^d	−7.606^e

^{a}C_nZn_2D: Zinc(II)–zinc(II) porphyrin dimer linked with alkoxy chain –O(CH$_2$)$_n$O–.
^{b}$\Delta\delta_{C_nZn_2D}(=\delta_{binding}-\delta_{C_nZn_2D})$: chemical shift change of C_nZn_2D after its binding with DABCO ([porphyrin]/[DABCO] = 1:1).
^{c}δ value of DABCO is 2.791.
^{d}δ value of DABCO in the presence of C_nZn_2D.
^{e}$\Delta\delta=\delta_{binding}-\delta_{DABCO}$: chemical shift change of DABCO after its binding with C_nZn_2D ([porphyrin]/[DABCO] = 1:1).
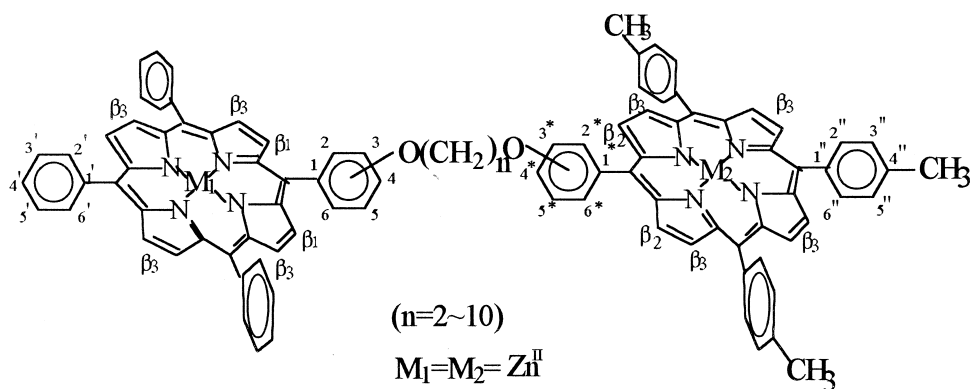
Fig. 4. Numbering system of NMR study of zinc(II)–zinc(II) porphyrin dimers $C_n Zn_2 D$.

of the inactive μ-OXO dimers. Therefore, the porphyrin dimers having ternary conformations have higher turnovers even than twice of that of FeTPPCl (2×5.02).

3.3. NMR study for zinc(II)–zinc(II) porphyrin dimers $C_n Zn_2 D$ and their binding behavior with 1 equiv. DABCO

Form Table 1 and Fig. 2, it can be supposed that the closed sandwich conformation has great influence on the catalytic activities of binuclear porphyrin dimers with the addition of 1 equiv. DABCO. It is well known that NMR study is an important and direct method to investigate the steric conformations of porphyrin dimers and polymers [12]. Because the paramagnetism of ferric ion, it is really difficult to get the satisfied NMR spectra of iron(III)–iron(III) porphyrin dimers. In order to look for the NMR evidence for the conformation effect on the catalytic hydroxylation, we synthesized a series of corresponding zinc(II)–zinc(II) porphyrin dimers, which were similar to the iron(III)–iron(III) porphyrin dimers described above except the difference of metal ion, the conformation of these zinc(II)–zinc(II) dimers with different alkoxy chain and their 1:1 binding behavior with DABCO have been studied by using ^{1}H-NMR spectroscopy.

Chemical shift values of zinc(II)–zinc(II) porphyrin dimers and the chemical shift changes

after they bind with DABCO, $\Delta \delta = \delta_{binding} - \delta_{C_n Zn_2 D}$, are summarized in Table 2, the individual resonances have been unambiguously assigned by use of ^{1}H$-^1$H COSY, the signals systems for zinc(II)–zinc(II) porphyrin dimers are shown in Fig. 4.

From Table 2, it has been shown that with the increase of the length of the alkoxy chain, all the chemical shifts of protons of meso β-H, phenyl and tolyl group of porphyrin rings of $C_n Zn_2 D$ move to upfield. These changes result from the ring current effect caused by the closed conformation of the two porphyrin rings of $C_n Zn_2 D$. When protons are above and below
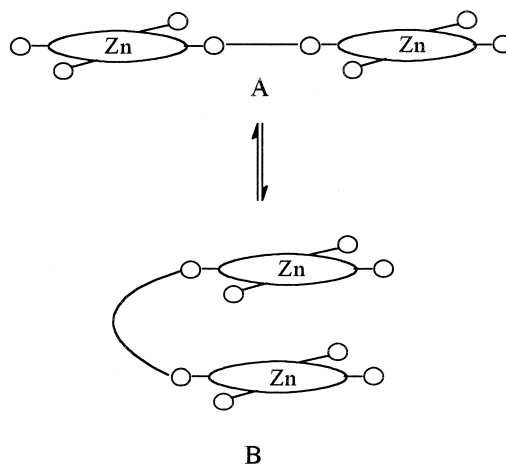

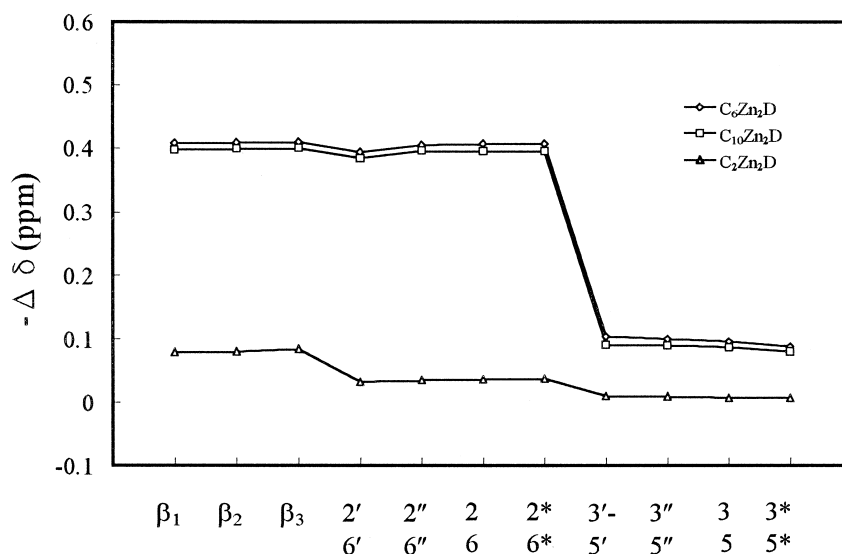Fig. 5. Conformation equilibrium of zinc(II)–zinc(II) porphyrin dimers.

Fig. 6. Plots of the chemical shift changes ($-\Delta\delta$) vs. porphyrin dimer protons.

the ring current of large conjugated π bond of porphyrin ring, the shielding effect causes their chemical shifts move to upfield. When protons are outside the ring current, they are influenced by deshielding effect and their chemical shifts move to downfield [13,14]. The data of Table 2 reveal that with the increase of the length of alkoxy chain, the conformation equilibrium of C_nZn_2D gradually moves from open to the closed conformation (Fig. 5).

From Table 2, it is worth noting that after the 1:1 binding behaviors of C_nZn_2D and DABCO, chemical shifts of both protons of zinc(II)–zinc(II) porphyrin dimers and DABCO move to upfield, all these results mean the formation of stable ternary sandwich complex. In these cases, the ring current effect of two cofacial porphyrin π systems causes the upfield shifts of protons of porphyrins, since DABCO is inside two porphyrin rings, the strong shielding effect of two porphyrin π systems causes its signals move greatly to upfield [15]. The plot of $\Delta\delta$ value ($\Delta\delta = \delta_{\text{binding}} - \delta_{C_nZn_2D}$) vs. protons of zinc-(II)–zinc(II) porphyrin dimers are shown in Fig. 6. It is obvious that the $\Delta\delta$ curves of C_6Zn_2D and $C_{10}Zn_2D$ are quite similar and are larger

than that of C_2Zn_2D, indicating the length of their alkoxy chain may be suitable to form ternary sandwich complex (like Fig. 3B). For C_2Zn_2D dimer, shift value changes of porphyrin rings and DABCO are much smaller than that of C_6Zn_2D and $C_{10}Zn_2D$. The weak ring current effect proves that DABCO can hardly bind inside the cavity of C_2Zn_2D. Fig. 6 indicates that for porphyrin dimers with different alkoxy chain, the tendency to form the ternary complex is consistent with the order of their catalytic activities. Therefore, these NMR results conform that the catalytic activities of iron(III)–iron(III) porphyrin dimers are related to their special conformation binding with DABCO.

Acknowledgements

References

[1] K. Maruguma, A. Osuka, Pure Appl. Chem. 62 (1990) 1511.
[2] R.W. Wagner, T.E. Johnson, F.R. Li, J.S. Lindsey, J. Org. Chem. 60 (1995) 5266.
[3] H. Higuchi, K. Shimizu, J. Ojima, Tetrahedron Lett. 36 (1995) 5359.
[4] Y. Naruta, M. Sasayama, J. Chem. Soc. Chem. Commun. (1994) 2667.
[5] Q.Z. Ren, J.W. Huang, Z.L. Liu, L.N. Ji, S. Afr. J. Chem. 50 (1997) 181.
[6] J.W. Huang, Z.L. Liu, X.R. Gao, D. Yang, X.Y. Peng, L.N. Ji, J. Mol. Catal. A: Chem. 111 (1996) 261.
    Soc. 112 (1990) 5773.
[7] R.G. Little, J.A. Anton, P.A. Loach, J. Heterocycl. Chem. 12 (1975) 343.
[8] R.G. Little, J. Heterocycl. Chem. 15 (1978) 203.
[9] D. Mansuy, Pure Appl. Chem. 59 (1987) 759.
[10] R.B. Brookfield, H. Ellue, A. Harriman, J. Chem. Soc. Faraday Trans. 2 (81) (1985) 1837.
[11] Y. Kaizu, H. Maekawa, H. Kobagash, J. Phys. Chem. 90 (1986) 4234.
[12] L. Benthem, R.B.M. Koehorst, T.J. Schaafsma, Magn. Reson. Chem. 23 (1985) 732.
[13] R.J. Abraham, I. Marsden, Tetrahedron 48 (1992) 7489.
[14] K.J. Cross, M.J. Crossley, Aust. J. Chem. 45 (1992) 991.
[15] C.A. Hunter, M.N. Meah, J.K.M. Sanders, J. Am. Chem.